Flexural-Torsional Coupled Vibration of Slewing Beams Using Various Types of Orthogonal Polynomials

Rakesh K. Kapania
Department of Aerospace and Ocean Engineering,
Virginia Polytechnic Institute and State University,
Blacksburg, VA 24060, USA
Yong-Yook Kim*
Center for Healthcare Technology Development, Chonbuk National University,
Duckjin-dong, Duckjin-gu, Jeonju-si, Jeonbuk 561-756, Korea

Dynamic behavior of flexural-torsional coupled vibration of rotating beams using the Rayleigh-Ritz method with orthogonal polynomials as basis functions is studied. Performance of various orthogonal polynomials is compared to each other in terms of their efficiency and accuracy in determining the required natural frequencies. Orthogonal polynomials and functions studied in the present work are : Legendre, Chebyshev, integrated Legendre, modified Duncan polynomials, the special trigonometric functions used in conjunction with Hermite cubics, and beam characteristic orthogonal polynomials. A total of 5 cases of beam boundary conditions and rotation are studied for their natural frequencies. The obtained natural frequencies and mode shapes are compared to those available in various references and the results for coupled flexural-torsional vibrations are especially compared to both previously available references and with those obtained using NASTRAN finite element package. Among all the examined orthogonal functions, Legendre orthogonal polynomials are the most efficient in overall CPU time, mainly because of ease in performing the integration required for determining the stiffness and mass matrices.

Key Words : Natural Frequency, Rotating Blade, Rayleigh-Ritz Method, Orthogonal Polynomials, Flexural-Torsional Coupled Vibration

1. Introduction

Flexural-torsional coupled vibration of a rotating structure can occur in many engineering applications such as slewing robot arms, turbomachinery blades, aircraft propellers, helicopter rotors, and spinning spacecraft. To design these components, the dynamic characteristic, especially near resonant condition, need to be well examined to assure a safe operation. Among the dynamic characteristics of these structures, determining the natural frequencies and associated mode shapes are of fundamental importance in the study of resonant responses, aeroelasticity, and for forced vibration analysis. An accurate prediction of the forced response is usually very difficult because of the uncertainty of the excitation. Moreover, under the resonance conditions, what limits the vibration amplitude is the amount of damping available. In most cases, the damping is almost entirely aerodynamic and its assessment is just as uncertain as the excitation. Thus, classic design practice for such structures has been mainly to rely on the knowledge of the natural

* Corresponding Author,
E-mail : yykim@chonbuk.ac.kr
TEL : +82-10-2635-6245; **FAX** : +82-63-275-6245
Center for Healthcare Technology Development, Chonbuk National University, Duckjin-dong, Duckjin-gu, Jeonju-si, Jeonbuk 561-756, Korea. (Manuscript **Received** September 16, 2005; **Revised** August 21, 2006)

frequencies to avoid anticipated resonances.

Flexural-torsional coupled vibration occurs when the centroid and the shear center of the cross section of a beam do not coincide. The lack of coincidence between the centroid and the shear center occurs when the beam has less than two axis of symmetry or has anisotropy in the material. This makes the elastic axis different from the centroidal axis and thus causes torsional vibration when flexural vibrations occur. The flexural-torsional coupled vibration can be analyzed by combining one of the beam theories for bending with a torsional theory and a consideration of the various warping effects. The simplest model for the analysis of coupled bending and torsional vibration is combining the classical Bernoulli-Euler theory for bending and St. Venant theory for torsion (Bishop et al., 1989). Inclusion of a warping effect, Bishop Cannon and Miao (1989), results in a better approximation, especially for higher modes. Also, Bercin and Tanaka (1997) showed that for non slender beams, applying the Timoshenko Beam theory instead of the Bernoulli-Euler theory along with the inclusion of a warping effect can improve the accuracy for higher modes.

Centrifugal force on rotating structure affects dynamic characteristic of the structure by inducing additional stiffness. At high rotational speeds, centrifugal forces of considerable magnitude results in an additional stiffening of the beam, thus increasing the natural frequencies of the structure. There are two more forces induced by inertia force in a rotating beam. Young and Liou (1992) identified these two forces as the Coriolis force and the gyroscopic force. However, the effect of these two forces on the dynamic characteristic is insignificant compared to the effect induced by the centrifugal force. The numerical results of Leissa and Co (1984) on the rectangular cantilever plates show that the Coriolis force has an insignificant effect upon the natural frequencies if the angular speed is less than the first natural frequency of the configuration. The present work thus only focuses on the influence of centrifugal forces on the natural frequencies of a thin-walled beam.

When obtaining the natural frequencies and the mode shapes, the Rayleigh-Ritz method is a good candidate for analysis, both because of its simplicity and its ability to give good results with relatively less effort. The method requires a linear combination of assumed deflection shapes of structures in free harmonic vibration which satisfy at least the geometrical or kinematical boundary conditions of the vibrating structure. The results from the Rayleigh-Ritz method depend directly on how closely the assumed shape functions resemble the actual mode shapes. When an assumed shape function contributes to several modes, or when some modes are not represented in the assumed shape functions, then it is difficult to draw definite conclusions from the Rayleigh-Ritz results.

This study presents some insight into the nature of the natural frequency values, as obtained by the Rayleigh-Ritz method and their dependence on the nature of the assumed shape functions.

The choice of the admissible functions is very important to simplify the calculations and to guarantee convergence to the exact solution. As basis functions for the Rayleigh-Ritz method, orthogonal polynomials enable the computation of higher natural frequencies of any order to be accomplished without facing any numerical difficulties arising from the ill-conditioning of the matrices like the ones encountered by Singhvi and Kapania (1994) when simple polynomials were used as the basis functions.

The theory of orthogonal polynomials has been well established but the developments in constructive, computational, and software aspects are still in an early stage (2005). Nonetheless, there has been many efforts to use orthogonal polynomials in structural analysis mainly for normal mode analysis. Parasher et al.(2004) used orthogonal polynomials to obtain modal properties of piezoceramic cantilever beams. Liew et al.(2003) applied orthogonal polynomials as trial displacement functions for the analysis of thin, rectangular plates with central cut-outs. Houmat (2005) used the shifted Legendre orthogonal polynomials as shape functions for triangular elements in h-p version of the finite element method to analyze the vibration of membranes. As can be seen

from various literatures, many kinds of orthogonal polynomials can be used. However, the studies on the performance the comparison of various polynomials has been somewhat lacking.

The main objective of the present work is to study the development and analysis of the flexural-torsional vibration of beams and discover the effect of using orthogonal functions in obtaining natural frequencies of structures experiencing flexural-torsional coupled vibration. To find most appropriate approximating orthogonal function to be used in Ritz method, 7 types of orthogonal functions are examined and compared for their use as basis functions. The functions considered are: Legendre, Chebyshev, integrated Legendre, modified Duncan polynomials, the special trigonometric functions used in conjunction with Hermite cubics, and beam characteristic orthogonal polynomials. The orthogonal polynomials are used in the analysis of the coupled flexural-torsional vibration of rotating and non-rotating beams. The results are compared to those given in available references and for the case of coupled flexural-torsional vibrations of Euler-Bernoulli beam, these are compared to references and those obtained using the NASTRAN finite element package.

2. Equations of Motion and Boundary Conditions

A beam that displays flexural-torsional vibration is shown in Fig. 1. The equations of motion of a uniform beam executing coupled free bending and torsional vibration with warping, given in Bishop et al. (1983), are:

$$EI\frac{\partial^4 v}{\partial x^4}+m\frac{\partial^2(v+e\theta)}{\partial t^2}=0 \tag{1}$$

$$EI_w\frac{\partial^4\theta}{\partial x^4}-GJ\frac{\partial^2\theta}{\partial x^2}+m\frac{\partial^2[(e^2+r^2)\theta+ev]}{\partial t^2}=0 \tag{2}$$

Here, t denotes time, x is the distance along the elastic axis of the beam and v is the bending displacement of the shear center in the direction of the y axis, the beam cross-section being assumed symmetrical about the xz-plane, θ is the angle of twist, e the position of the section centroid C relative to the shear center S, m is the mass per unit length and r the polar radius of gyration of the cross-section about the centroid. The flexural rigidity with respect to the z-axis is EI, while EI_w is the torsional rigidity associated with warping and GJ is the Saint-Venant torsional rigidity.

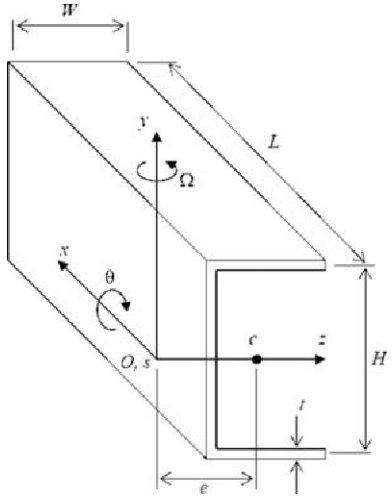

Fig. 1 A uniform channel beam

The boundary conditions are: at a clamped end $(x=0)$,

$$v=0=\frac{\partial v}{\partial x} \text{ and } \theta=0=\frac{\partial\theta}{\partial x} \tag{3}$$

at a free end $(x=L)$,

$$\frac{\partial^2 v}{\partial x^2}=0,\ \frac{\partial^3 v}{\partial x^3}=0,\ \frac{\partial^2\theta}{\partial x^2}=0,$$
$$\text{and } -EI_w\frac{\partial^3\theta}{\partial x^3}+GJ\frac{\partial\theta}{\partial x}=0 \tag{4}$$

When the beam rotates, the centrifugal force of $\Omega^2\int_x^L\rho A\zeta d\zeta$ (ρ is the material density and Ω is the rotating speed) is applied in axial direction. The effect of this axial force in the equation of motion is considered as was done by Banerjee and Fisher (1992). The equations of motions (1) and (2) become:

$$EI\frac{\partial^4 v}{\partial x^4}-m\Omega^2\int_x^L\zeta d\zeta\frac{\partial^2 v}{\partial x^2}+m\Omega^2 e\int_x^L\zeta d\zeta\frac{d^2\theta}{dx}$$
$$+m\frac{\partial^2 v}{\partial t^2}-me\frac{\partial^2\theta}{\partial t^2}=0 \tag{5}$$

$$m\Omega^2 e\int_x^L \zeta d\zeta \frac{\partial^2 v}{\partial x^2}+EI_w\frac{\partial^4\theta}{\partial x^4}-GJ\frac{\partial^2\theta}{\partial x^2} -m\Omega^2(e^2+r^2)\int_x^L \zeta d\zeta \frac{\partial^2\theta}{\partial x^2} -me\frac{\partial^2 v}{\partial t^2}+m(e^2+r^2)\frac{\partial^2\theta}{\partial t^2}=0 \tag{6}$$

Note that the governing equations become somewhat complex in the presence of centrifugal force.

3. Derivation of Mass and Stiffness Matrices

We assume the solution of the differential equations (5) and (6) to be in the form of

$$v(x,t)=V(x)\,e^{-i\omega t} \tag{7}$$

$$\theta(x,t)=\Theta(x)\,e^{-i\omega t} \tag{8}$$

where ω denotes the frequency of natural flexural-torsional coupled motion, and $V(x)$ and $\Theta(x)$ denotes mode shapes during the vibration. Substitution of Eqns. (7) and (8) into Eqns. (5) and (6) gives

$$\left[EI\frac{d^4V}{dx^4}-m\Omega^2\int_x^L \zeta d\zeta\left(\frac{d^2V}{dx^2}-e\frac{d^2\Theta}{dx^2}\right) -\omega^2(mV-me\Theta)\right]e^{-i\omega t}=0 \tag{9}$$

$$\left[m\Omega^2\int_x^L \zeta d\zeta\left\{e\frac{d^2V}{dx^2}-(e^2+r^2)\frac{d^2\Theta}{dx^2}\right\} +EI_w\frac{d^4\Theta}{dx^4}-GJ\frac{d^2\Theta}{dx^2} -\omega^2\{m(e^2+r^2)\Theta-meV\}\right]e^{-i\omega t}=0 \tag{10}$$

The weak forms are derived by multiplying Equation (9) with a weight function w_1 and Equation (10) with a weight function w_2 and integrating the resulting equations over the beam length. Replace ω^2 by λ and the weak forms, Eqs. (9) and (10), respectively become:

$$\int_0^L w_1\left\{EI\frac{d^4V}{dx^4}-m\Omega^2\int_x^L \zeta d\zeta\left(\frac{d^2V}{dx^2}-e\frac{d^2\Theta}{dx^2}\right) -\omega^2(mV-me\Theta)\right\}dx=0 \tag{11}$$

$$\int_0^L w_2\left[m\Omega^2\int_x^L \zeta d\zeta\left\{e\frac{d^2V}{dx^2}-(e^2+r^2)\frac{e^2\Theta}{dx^2}\right\} +EI_w\frac{d^4\Theta}{dx^4}-GJ\frac{d^2\Theta}{dx^2}-\lambda\{m(e^2+r^2)\Theta-meV\}\right]dx=0 \tag{12}$$

Using integration by parts twice, the order of differentiation of the weight function and the dependent variable is distributed evenly.

$$\int_0^L\left\{EI\frac{d^2w_1}{dx^2}\frac{d^2V}{dx^2}+m\Omega^2\int_x^L \zeta d\zeta\left(\frac{dw_1}{dx}\frac{dV}{dx}-e\frac{dw_1}{dx}\frac{d\Theta}{dx}\right) -\lambda(mw_1V-mew_1\Theta)\right\}dx +w_1\left\{EI\frac{d^3V}{dx^3}-m\Omega^2\int_x^L \zeta d\zeta\left(\frac{dV}{dx}-e\frac{d\Theta}{dx}\right)\right\}\Big|_0^L -\frac{dw_1}{dx}\left(EI\frac{d^2V}{dx^2}\right)\Big|_0^L=0 \tag{13}$$

$$\int_0^L\left\{EI_w\frac{d^2w_2}{dx^2}\frac{d^2\Theta}{dx^2}+m\Omega^2\int_x^L \zeta d\zeta\left(e\frac{dw_2}{dx}\frac{dV}{dx}-(e^2+r^2) -\frac{dw_2}{dx}\frac{d\Theta}{dx}\right)+GJ\frac{dw_2}{dx}\frac{d\Theta}{dx}-\lambda\{m(e^2+r^2)w_2\Theta-mew_2V\}\right\}dx -w_2\left\{m\Omega^2\int_x^L \zeta d\zeta\left(e\frac{dV}{dx}-(e^2+r^2)\frac{d\Theta}{dx}\right)-EI_w\frac{d^3\Theta}{dx^3}+GJ\frac{d\Theta}{dx}\right\}\Big|_0^L -\frac{dw_2}{dx}EI_w\frac{d^2\Theta}{dx^2}\Big|_0^L=0 \tag{14}$$

From Eqs. (13) and (14), primary variables are identified as V, dV/dx, Θ, $d\Theta/dx$. Therefore V and Θ have to fulfill essential boundary conditions for the fixed end. Using the essential and natural boundary conditions, given in Eqs. (3) and (4), the weak forms reduce to,

$$\int_0^L\left\{EI\frac{d^2w_1}{dx^2}\frac{d^2V}{dx^2}+m\Omega^2\int_x^L \zeta d\zeta\frac{dw_1}{dx}\frac{dV}{dx} -m\Omega^2e\int_x^L \zeta d\zeta\frac{dw_1}{dx}\frac{d\Theta}{dx}-\lambda(mw_iV-mew_i\Theta)\right\}dx=0$$

$$\int_0^L\left\{EI_w\frac{d^2w_2}{dx^2}\frac{d^2\Theta}{dx^2}-m\Omega^2e\int_x^L \zeta d\zeta\frac{dw_2}{dx}\frac{dV}{dx} +GJ\frac{dw_2}{dx}\frac{d\Theta}{dx}-m\Omega^2(e^2+r^2)\int_x^L \zeta d\zeta\frac{dw_2}{dx}\frac{d\Theta}{dx} -\lambda\{m(e^2+r^2)w_2\Theta-mew_2V\}\right\}dx=0 \tag{15}$$

In the Rayleigh-Ritz method, we seek an approximate solution to Eq. (15) in the form of a finite series:

$$V_m=\sum_{j=1}^m v_j\Psi_j^{(1)}+\Psi_0^{(1)} \tag{16}$$

$$\Theta_n=\sum_{j=1}^n \theta_j\Psi_j^{(2)}+\Psi_0^{(2)} \tag{17}$$

where Ψ_0, Ψ_1, Ψ_2, $\cdots$ are approximating functions and v_j and θ_j are the undetermined parameters. In the Rayleich Ritz method, Functions Ψ_0 fulfill the

specified nonhomogeneous essential boundary conditions and $\Psi_1, \Psi_2, \cdots$ satisfy at least the homogeneous form of the essential boundary conditions. In the present work, orthogonal functions are used as approximating functions. To express Eq. (15) in the matrix form, we substitute V_m and Θ_n for V and $\psi_i^{(1)}$ and $\psi_i^{(2)}$ and for w_1 and w_2, respectively. The stiffness and mass matrices are as follows:

$$\begin{bmatrix}[K^{11}] & [K^{12}] \\ [K^{12}] & [K^{22}]\end{bmatrix}\begin{Bmatrix}\{A\} \\ \{B\}\end{Bmatrix}-\lambda\begin{bmatrix}[M^{11}] & [M^{12}] \\ [M^{12}] & [M^{22}]\end{bmatrix}\begin{Bmatrix}\{A\} \\ \{B\}\end{Bmatrix} =\begin{Bmatrix}\{0\} \\ \{0\}\end{Bmatrix} \tag{18}$$

where

$$K_{ij}^{11}=\int_0^L\left\{EI\frac{d^2\Psi_i^{(1)}}{dx^2}\frac{d\Psi_j^{(1)}}{dx^2}+m\Omega^2\int_x^l\zeta d\zeta\frac{d\Psi_i^{(1)}}{dx}\frac{d\Psi_j^{(1)}}{dx}\right\}dx \tag{19}$$

$$K_{ij}^{12}=-\int_0^L m\Omega^2 e\int_x^L\zeta d\zeta\frac{d\Psi_i^{(1)}}{dx}\frac{d\Psi_j^{(2)}}{dx}dx \tag{20}$$

$$K_{ij}^{22}=\int_0^L\left\{EI_w\frac{d^2\Psi_i^{(2)}}{dx^2}\frac{d^2\Psi_j^{(2)}}{dx^2}+GJ\frac{d\Psi_i^{(2)}}{dx}\frac{d\Psi_j^{(2)}}{dx}+m\Omega^2(e^2+r^2)\int_x^L\zeta d\zeta\frac{d\Psi_i^{(2)}}{dx}\frac{d\Psi_j^{(2)}}{dx}\right\}dx \tag{21}$$

$$M_{ij}^{11}=\int_0^L\rho A\psi_i^{(1)}\Psi_j^{(1)}dx \tag{22}$$

$$M_{ij}^{12}=-\int_0^L\rho Ae\Psi_i^{(1)}\Psi_j^{(2)}dx \tag{23}$$

$$M_{ij}^{22}=\int_0^L\rho A(e^2+r^2)\Psi_i^{(2)}\Psi_j^{(2)}dx \tag{24}$$

The integrations for each terms in mass and stiffness matrices were performed using MATHEMATICA (Wolfram Research Co., USA) when orthogonal polynomials were used as approximating functions.

4. Approximating Functions

When using the Rayleigh-Ritz method, approximating functions have to fulfill essential boundary conditions. In the case of bending-torsion coupled beam, essential boundary conditions showin in Eq. (3) have to be fulfilled at the clamped base. However, Legendre and Chebyshev orthogonal polynomials by themselves do not fulfill all these essential boundary conditions while still retaining their orthogonality. To fulfill these essential boundary conditions, artificial linear and rotational springs are introduced in the stiffness matrix and even order Legendre and Chebyshev polynomials are used. The reason that only the even order polynomials are chosen is that the even order polynomials fulfill the essential boundary conditions of a cantilever beam. The additional stiffness terms to enable Legendre and Chebyshev polynomials to be used in the analysis are $1/2\alpha v(0)^2$, $1/2\beta v'(0)^2$, $1/2\gamma\theta(0)^2$, and $1/2\partial\theta'(0)^2$, where α, β, γ, and ζ are the artificial spring stiffnesses. To simulate cantilever conditions, a large numerical value (up to 10^{10}) is chosen for the stiffness of artificial springs.

Integrated Legendre polynomial is a linear combination of two integrals of Legendre polynomials. The first and second terms are linear combinations of two integrals of Legendre polynomials.

$$I_2(x)=\frac{(1+x)}{2}\qquad I_1(t)=\frac{(1-x)}{2} \tag{25}$$

The rest of the polynomials $I_n(t)$ are found from the relationship obtained by Szab (and Babuska (1991) as:

$$I_n(x)=\frac{1}{\sqrt{2(2n-3)}}(p_{n-1}(x)-p_{n-3}(x)),\quad (n\geq 3) \tag{26}$$

where $P_n(x)$ are Legendre polynomials. To fulfill essential boundary conditions of cantilever beam at $x=0$ in cantilever Euler-Bernoulli beam, integrated Legendre Polynomials are modified to be

$$J_n(x)=I_n(x)-I_n(0),\ n=3,\ 5,\ \cdots \tag{27}$$

The modified Duncan polynomials of Karunamoorthy, Peters, and Barwey (1993) are obtained by orthogonalizing Duncan trinomials by using Gram-Schmidt process. Duncan polynomials for bending are

$$Y_n=\frac{1}{6}(n+2)(n+3)x^{n+1}-\frac{1}{3}n(n+3)n^{n+2}+\frac{1}{6}n(n+1)x^{n+3} \tag{28}$$

for $n=1, 2, 3, \cdots$ satisfy the boundary conditions for a cantilever beam and are complete and lin-

early independent. These polynomials are orthogonalized in the interval 0 to 1 by the Gram-Schmidt orthogonalization process and scaled so that the tip deflection is unity $Y_n(1)=1$. The orthogonalized polynomials also satisfy the boundary conditions for a cantilever beam.

Bardell, Dudson, and Langley (1993) use the special trigonometric functions in conjunction with Hermite cubics. The trigonometric functions used as hierarchical functions are

$$f_r(x)=\sin\left(\frac{\pi}{2}(r-4)\,(x+1)\right)\sinh\left(\frac{\pi}{2}(x+1)\right) \quad (29)$$

Bhat's beam characteristic orthogonal polynomials (Bhat, 1986) consist of choosing a first polynomial $\phi_1(x)$ which satisfies both the geometrical and the natural boundary conditions of a uniform beam and obtaining the other members of the orthogonal set in the interval by using the Gram-Schmidt process as follows:

$$\begin{aligned}&\phi_2(x)=(x-B_2)\,\phi_1(x),\ \cdots,\\&\phi_k(x)=(x-B_k)\,\phi_{k-1}(x)-C_k\phi_{k-2}(x)\end{aligned} \quad (30)$$

$$B_k=\frac{\int_a^b xw(x)\,\phi_{k-1}^2(x)\,dx}{\int_a^b w(x)\,\phi_{k-1}^2(x)\,dx}$$

where

$$C_k=\frac{\int_a^b xw(x)\,\phi_{k-1}(x)\,\phi_{k-2}(x)\,dx}{\int_a^b w(x)\,\phi_{k-2}^2(x)\,dx}$$

where $w(x)$ is the weighting function that is unity for uniform beams. When $\phi_1(x)$ satisfies both geometrical and natural boundary conditions, the additional polynomials generated by Gram-Schmidt orthogonalization satisfy only the geometric boundary conditions.

5. Results

Orthogonal functions mentioned in the previous section are examined for their respective performance as the basis functions for the Rayleigh-Ritz method employed to find the natural frequencies of both non-rotating and rotating beams. MATHEMATICA is used in generating the mass and the stiffness matrices and getting eigenvalues for natural frequencies in the Rayleigh-Ritz method. The analysis was done using Silicon Graphics Octane workstation. For the reference purpose, the results for a channel beam cases, obtained using NASTRAN, are compared with the present results.

5.1 A cantilever case

For the case of coupled bending-torsion vibration of a cantilever beam, most of the orthogonal functions used show very good agreements, as seen in Table 1 to the reference which also uses Euler-Bernoulli beam theory for bending. For Legendre and Chebyshev polynomials cases, artificial spring of stiffness 10^7 is added to the stiffness term of (18) and (20). Figures 2 and 3 show mode shapes obtained by NASTRAN. Among orthogonal functions used in the analysis, beam

Table 1 The natural frequencies of coupled flexural torsional vibration of a short cantilever beam (750 CQUAD4 elements used in the NASTRAN analysis, Channel Dimensions: H=0.8 m, W=0.05 m, t=0.005 m, L=3.2 m)

Polynomials	1	2	3	4	5	N	T (sec)	Integration
Bercin and Tanaka (1997)	24.03	88.54	131.41	358.57	549.83			
Legendre	24.03	88.45	131.64	360.34	550.21	10	34.5	Symbolic
Chebyshev	24.03	88.45	131.64	360.34	550.21	10	55.2	〃
Integrated Legendre	24.03	88.45	131.58	359.84	549.93	10	56.5	〃
Modified Duncan	24.02	88.44	131.4	358.55	549.21	10	122.6	〃
Beam Characteristic	24.03	88.44	131.44	366.62	549.49	5	284.4	〃
Bardell's functions	24.24	89.55	131.48	358.84	549.53	10	497.2	Numerical
NASTRAN	22.91	84.55	126.3	390.01	555.40	FEM		

characteristic orthogonal polynomials show most close approximations. Natural frequencies obtained by NASTRAN also show some deviation from the results given in the reference and from the results obtained from the present results. This seems to be due to the fact that the elements used in the NASTRAN analysis are 2-dimensional plate elements and allow all types of complicating effects such as the shear deformation and rotatory inertia along with a better representation of the warping effect.

5.2 A rotating cantilever case

Natural Frequencies of the flexural-torsional coupled vibration of a rotating, cantilever, Bernoulli-Euler Channel Beam are shown in Table 2. For each case, 10 polynomials were used as approximating functions. Also, the highest order of polynomials used is 20 in the case of Chebyshev and Legendre polynomials because only even numbers of polynomials were used. For the integrated Legendre polynomial case, the odd order polynomials were also used and the hig-

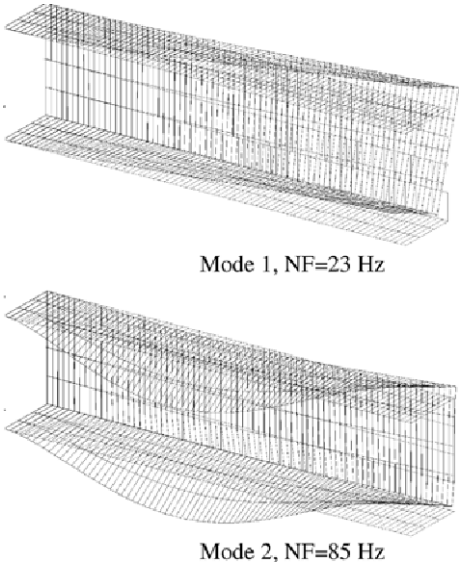

Fig. 2 Mode shapes for the first and second modes of a short cantilever channel beam obtained using NASTRAN (1216 CQUAD4 elements)

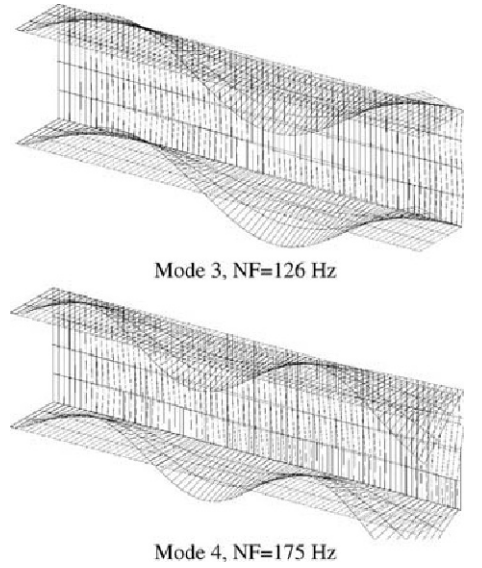

Fig. 3 Mode shapes for the third and fourth modes of a short cantilever channel beam obtained using NASTRAN (1216 CQUAD4 elements)

Table 2 Natural frequencies of a flexural-torsional coupled vibration of a rotating slender cantilever beam (Ω=600 rpm, 392 CQUAD4 elements used in the NASTRAN analysis, channel specifications from Bishop, Price, and Zhang, 1983, Channel Dimensions: H=12.7 mm, W=25.4 mm, t=0.635 mm, L=1.016 m)

Polynomials	1	2	3	4	5	N	T (sec)	Integration
Legendre	15.802	55.397	123.519	220.014	351.397	10	36.9	Symbolic
Chebyshev	15.708	56.241	123.317	219.823	351.207	10	53.8	〃
Integrated Legendre	15.862	56.32	126.293	225.34	358.124	10	55	〃
Modified Duncan	15.77	55.386	122.891	217.854	343.495	10	120.5	〃
Beam Characteristic	15.77	55.373	122.754	217.659	343.423	10	216.9	〃
Bardell's functions	16.135	56.695	126.382	224.91	355.337	10	517.3	Numerical
NASTRAN	15.755	46.738	114.505	199.538	304.306	FEM		

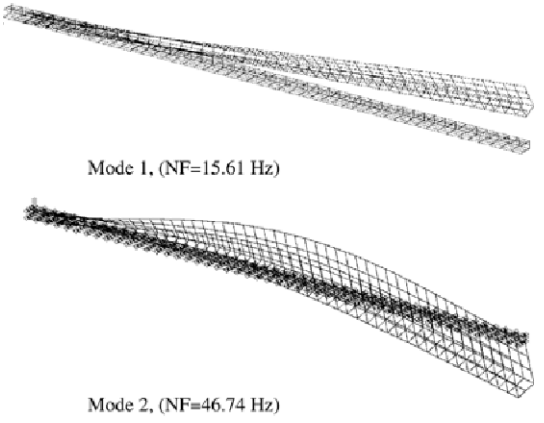

Fig. 4 Mode shapes for the first and second modes of a rotating cantilever channel beam obtained using NASTRAN (Ω=600 rpm, 8475 CQUAD4 elements)

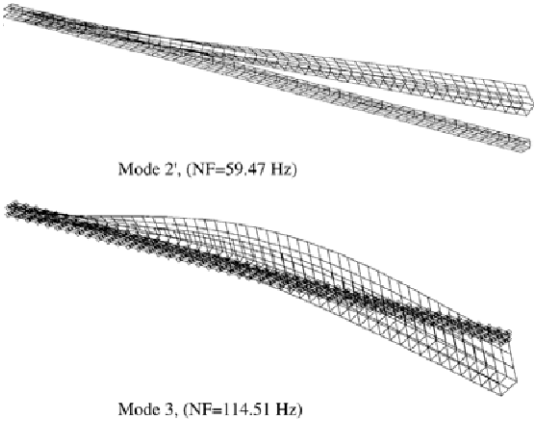

Fig. 5 Mode shapes for the "second" and third modes of a rotating cantilever channel beam obtained using NASTRAN (Ω=600 rpm, 8475 CQUAD4 elements)

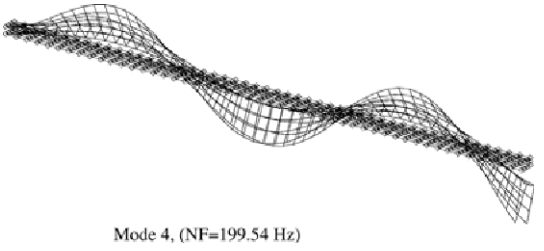

Fig. 6 Mode shapes for the fourth mode of a rotating cantilever channel beam obtained using NASTRAN (Ω=600 rpm, 8475 CQUAD4 elements)

hest order was 19. In the cases of beam characteristic and Karunamoorthy's modified Duncan polynomials, these polynomials of the order of 4 through 13 were used. Figures 4 through 6 show mode shapes, for first through fourth modes, obtained using NASTRAN. Figure 5 shows another mode between the second mode and the third mode. However this seems to be twist only mode when compared to other mode shapes. Figures 7 and 8 show mode shapes obtained for different approximating functions. These figures show that there are some differences between mode shapes obtained with NASTRAN and those obtained with various orthogonal functions. However, the results obtained using orthogonal polynomials show close agreement with respect to each other. Beam characteristic orthogonal polynomials show the closest approximations to the NASTRAN results when we see Table 2. However, the beam

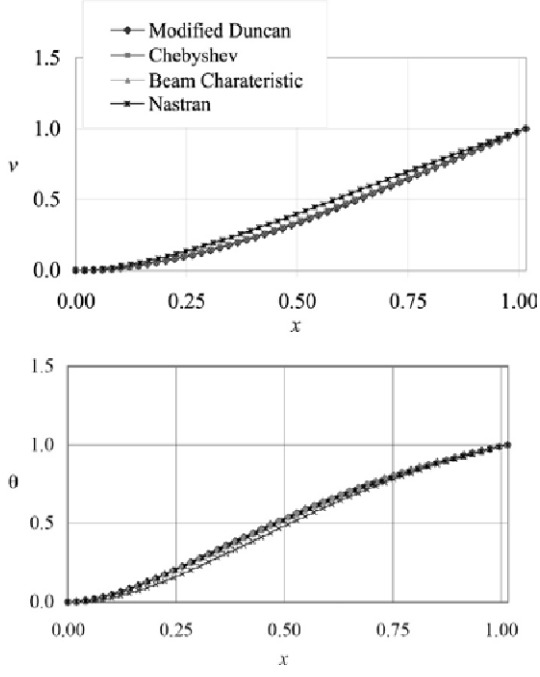

Fig. 7 The comparison of the first mode shapes obtained with Rayleigh–Ritz method using various approximating functions and Nastran mode shapes obtained with the NASTRAN plate elements for a rotating bending–torsion couopled slender cantilever channel beam (Ω=600 rpm)

characteristic polynomials require a significant amount of computational time in getting the coefficients of polynomials and generating the mass and the stiffness matrices by integration as the number of polynomials used are increased.

The reason that there are difference between mode shapes between the results obtained with the NASTRAN and the results obtained with various orthogonal polynomials is perhaps due to the fact that warpings are not well considered in the analysis with orthogonal polynomials. Figure 9 shows the side view of deformation at the tip on the 4th normal mode. The left Figure in Fig. 9 shows apparent effect of warping on the cross section but the effect is not seen in the section deformation when we see the side view seen as in the right figure in Fig. 9. Since warping stiffness is considered in the present analysis, the deviation of results is most probably due to missing mode which cannot be represented by orthogonal polynomials. Therefore, in the case of the rotating cantilever bending-torsion coupled beam, at least the first mode could be correctly found with the Rayleigh-Ritz method using orthogonal functions but other modes were overestimated.

In Fig. 9, natural frequencies obtained by different number of polynomials are shown. The case shown in the figure is the natural frequency of the fourth mode shape of the rotating bending-torsion coupled beam. In the figure, the results obtained using Chebyshev, Karunamoorthy's modified Duncan and beam characteristic orthogonal polynomials are compared to each other. Among

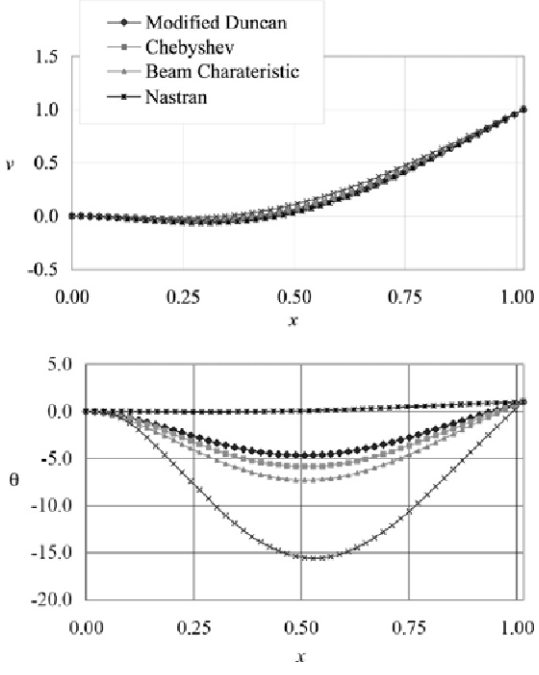

Fig. 8 The comparison of the mode shapes for the second mode obtained using various approximating functions and Nastran for a rotating bending-torsion coupled slender cantilever channel beam (Ω=600 rpm). Note the significant differences, in the amplitude of the mode shape for the angular motion, obtained for various polynomials

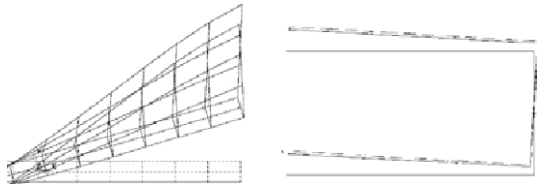

Fig. 9 Tip deformation shape in the 4th normal mode of a rotating bending-torsion coupled beam as obtained by the NASTRAN analysis (Ω=600 rpm)

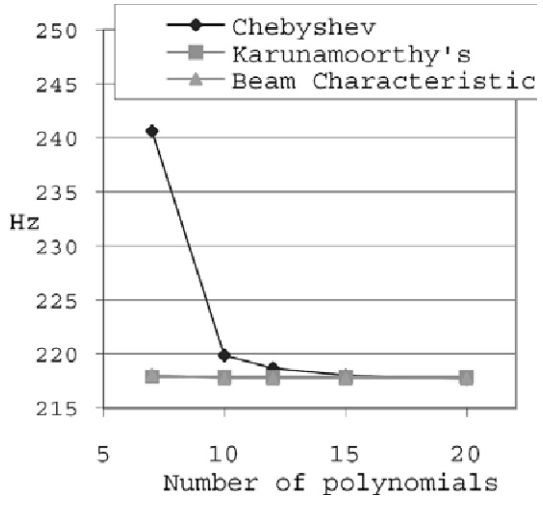

Fig. 10 Convergence results for the fourth mode, as obtained by using different number of polynomials, for coupled flexural-torsional vibration of a slender channel beam (Ω=600 rpm)

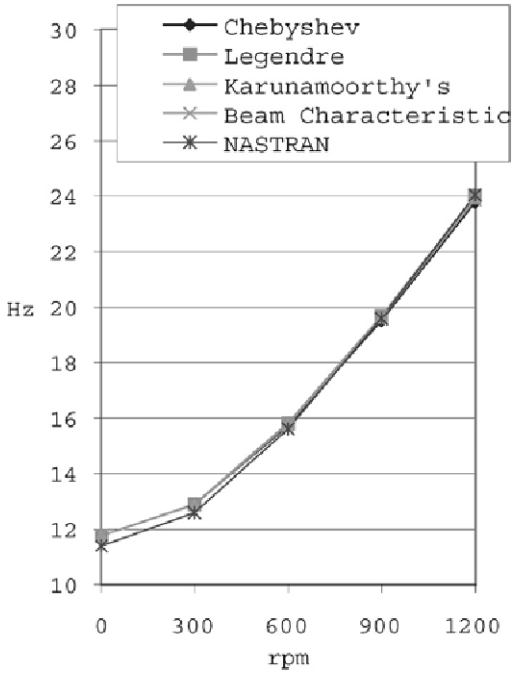

Fig. 11 Natural frequencies of the first mode of coupled flexural-torsional vibration for different rotating speeds

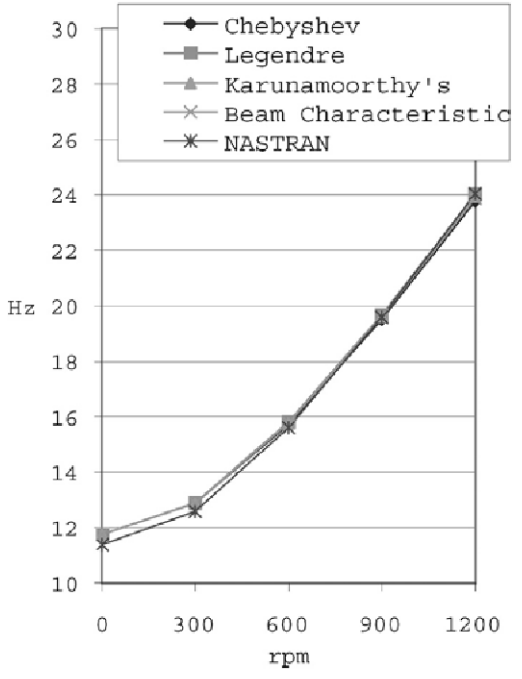

Fig. 12 Natural frequencies of the first mode of rotating coupled flexural-torsional vibration for different lengths in meters (Ω=600 rpm)

the orthogonal polynomials used, Karunamoorthy's modified Duncan polynomial and beam characteristic polynomials show a faster convergence than the Chebyshev polynomials which fulfill essential boundary condition approximately using the artificial springs.

To examine the effect of rotation, the natural frequencies of first mode shapes of coupled flexural-torsional vibration obtained using various polynomials are compared to each other in Fig. 11. The figure shows a close agreement between the results obtained using various polynomials. The results from the NASTRAN analysis show a slightly higher natural frequency at higher rotation speeds than the results obtained using the Ritz method employing various types of orthogonal polynomials.

Next, the natural frequencies for the coupled flexural-torsional vibration are obtained and compared, in Fig. 12 for different lengths of the rotating beam. The figure shows that natural frequencies obtained using NASTRAN analysis shows lower values than those using the Rayleigh-Ritz method for shorter beams. This seems to be due to the fact that shear and rotational inertia effects are better accounted in the NASTRAN analysis.

6. Summary and Conclusion

Various orthogonal polynomials were examined to evaluate their performance in determining the natural frequencies of normal modes in a rotating beam having bending-torsion coupling. Tested orthogonal polynomials show good approximations compared to other orthogonal functions which contain trigonometric functions in finding normal modes of non-rotating and rotating beams. Among tested orthogonal functions, simple Legendre polynomials gave best efficiency in getting results. This is mainly because the integration takes less time with these polynomials. Bardell's orthogonal functions, do not show good efficiency in getting results. This is mainly due to the enormous time consumed in the integration of the relevant functions when generating the mass and stiffness matrices. Also, these orthogonal functions give less accurate approximations compared

to orthogonal polynomials when the same number of approximating functions are used. Beam characteristic orthogonal polynomials show most accurate results and a faster convergence but they also require a significant calculation time in generating assumed mode polynomials for different boundary conditions.

The polynomials employed here can be extended to analyze natural modes of coupled vibrations including axial and lateral vibrations along with flexural-torsional vibrations. Furthermore, coupled vibrations of multi-cell composite thin-walled beams can be analyzed using the developed method. Moreover, more efficient method to fulfill essential boundary conditions and explicit addition of warping function in the strain-displacement relation should be explored in the future work.

Acknowledgements

Authours would like to thank the Regional Research Centers Program of the Korean Ministry of Education and Human Resources Development through the Center for Healthcare Technology Development.

References

Banerjee, J. R. and Fisher S. A., 1992, "Coupled Bending-Torsional Dynamic Stiffness Matrix for Axially Loaded Beam Elements," *International Journal for Numerical Methods in Engineering*, Vol. 33, pp. 739～751.

Bardell, N. S., Dunsdon, J. M., and Langley, R. S., 1993, "Free Vibration of Thin, Isotropic, Open, Conical Panels," *Journal of Sound and Vibration*, Vol. 217, No. 2, pp. 297～320.

Bercin, A. N. and Tanaka, M., 1997, "Coupled Flexural-Torsional Vibrations of Timoshenko Beams," *Journal of Sound and Vibration*, Vol. 207, No. 1, pp. 47～59.

Bhat, R. B., 1986, "Transverse Vibrations of a Rotating Uniform Cantilever Beam with Tip Mass as Predicted by Using beam Characteristic Orthogonal Polynomials in the Rayleigh-Ritz Method," *Journal of Sound and Vibration*, Vol. 105, No. 2, pp. 199～210.

Bishop, R. E. D., Cannon, S. M. and Miao, S., 1989, "On Coupled Bending and Torsional Vibration of Uniform Beams," *Journal of Sound and Vibration*, Vol. 131, No. 3, pp. 457～464.

Bishop, R. E. D., Price, W. G. and Zhang, X, 1983, "On the Structural Dynamics of a Vlasov Beam," *Proceedings of the Royal Society*, London, A388, 1983, pp. 49～73.

Gautschi, W., 2005, "Orthogonal Polynomias (in Matlab)," *Journal of Computational and Applied Mathematics*, Vol. 178, pp. 215～234.

Houmat, A., 2005, "Free Vibration Analysis of Membranes Using the h-p Version of the Finite Element Method," *Journal of Sound and Vibration*, Vol. 282, No. 1, pp. 401～410.

Karunamoorthy, S. N., Peters, D. A. and Barwey, D., 1993, "Orthogonal Polynomials for Energy Methods in Rotary Wing Structural Dynamics," *Journal of the American Helicopter Society*, Vol. 38, No. 3, pp. 93～98.

Leissa, A. W. and Co, C. M., 1984, "Coriolis Effects on the Vibrations of Rotating Beams and Plates," *Proceedings of Twelfth Southeastern Conference on Theoretical and Applied Mechanics*, pp. 508～513.

Liew, K. M., Kitipornchai, S., Leung, A. Y. T. and Lim, C. W., 2003, "Analysis of the Free Vibration of Rectangular Plates with Central Cut-Outs Using the discrete Ritz Method," *Internaitonal Journal of Mechanical Sciences*, Vol. 45, pp. 941～959.

Parashar, S. K., Wagner, U. V. and Hagedorn, P., 2004, "Nonlinear Shear-Induced Flexural Vibrations of Piezoceramic Actuators : Experiments and Modeling," *Journal of Sound and Vibration*, Vol. 285, No. 4, pp. 989～1104.

Singhvi, S. and Kapania, R. K., 1994, "Comparison of Simple and Chebyshev Polynomials in Rayleigh-Ritz Analysis," *Journal of Engineering Mechanics*, Vol. 120, No. 10, pp. 2126～2135

Szabo, B. and Babuska, I., 1991, *Finite Element Analysis*, John Wiley & Sons, New York.

Young, T. H. and Liou, G. T., 1992, "Coriolis Effect on the Vibration of a Cantilever Plate With Time-Varying Rotating Speed," *Journal of Vibration and Acoustics*, Vol. 114, pp. 232～241.